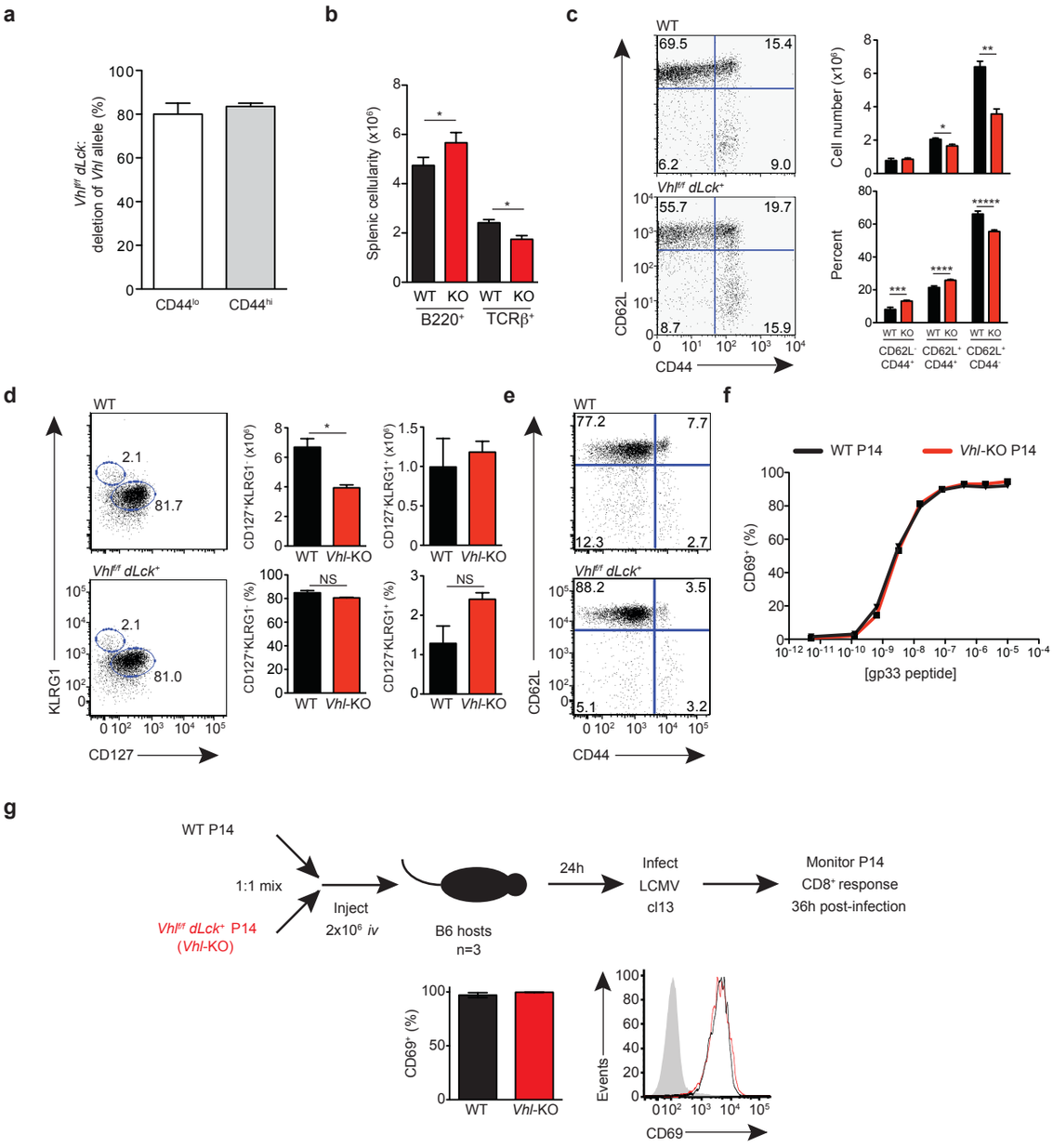

Supplementary Figure 1. Deletion of VHL, splenic composition, resting phenotype and TCR responsiveness for the *Vhl*$^{fl/lf}$ dLck model. (**a**) Deletion of VHL in gDNA from sorted CD44^{lo} and CD44^{hi} *Vhl*$^{fl/fl}$ dLck (VHL-KO) CD8$^+$ T cells relative to WT cells as determined by qPCR, n=2, error bars indicate range. (**b**) Absolute number of splenic B220$^+$ cells and TCRβ$^+$ cells for wild-type and VHL-KO mice; WT n=6, VHL-KO n=3. * P = 0.014 (Student's unpaired t-test). (**c**) Representative CD44 and CD62L phenotype of polyclonal CD8$^+$CD4$^-$ T cells and the absolute number and relative splenic percentage of indicated subsets; WT n=6, VHL-KO n=3, * P = 0.011, ** P = 0.0011, *** P = 0.033, **** P = 0.023 and ***** P = 0.006 (Student's unpaired t-test). (**d**) CD127 and KLRG1 phenotype of uninfected splenic polyclonal CD8$^+$CD4$^-$ T cells, number and %; n=3, derived from different mice than **c**; * P = 0.011 (Student's unpaired t-test). (**e**) CD44 and CD62L phenotype of splenic P14 (CD8α$^+$CD4$^-$Vα2$^+$) T cells from VHL-sufficient and VHL-deficient P14 TCR transgenic mice. (**f,g**) Equivalent TCR sensitivity/early activation of VHL-sufficient and VHL-deficient P14 T cells to a range of gp33 peptide *in vitro* and to LCMV clone 13 *in vivo*. (**f**) P14 VHL-sufficient or VHL-deficient splenocytes were mixed at a 1:1 ratio and the indicated amount of gp33 peptide was added to duplicate wells. Upregulation of CD69 on VHL-sufficient and VHL-deficient cells was assessed by flow cytometry using congenic markers to distinguish each population after 18 hrs of stimulation; representative of two independent experiments. (**g**) Experimental set up as in **f**, but the mixture of P14 CD8$^+$ T cells was transferred into B6 mice followed by infection with LCMV clone 13. Splenocytes were analyzed 36 hrs after infection. Grey-filled histogram indicates the fluorescence of naïve CD8$^+$ T cells from uninfected mice; n=3, representative of two independent experiments. Error bars indicate s.e.m.

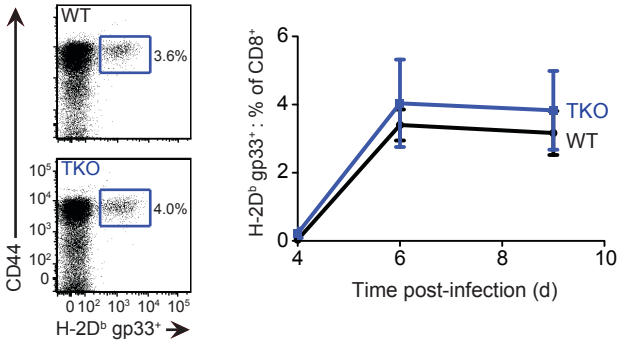

Supplementary Figure 2. Similar virus-specific CTL accumulation in T cell–specific triple VHL-HIF-1α-HIF-2α-deficient mice. Wild-type and VHL-HIF-1α-HIF-2α dLck mice were infected with LCMV clone 13. Frequency of H-2D^b gp33 tetramer-positive cells in the peripheral blood for representative samples on day 6 of infection (left) or at the time points indicated (right); n=3, error bars indicate s.e.m., representative of two experiments.

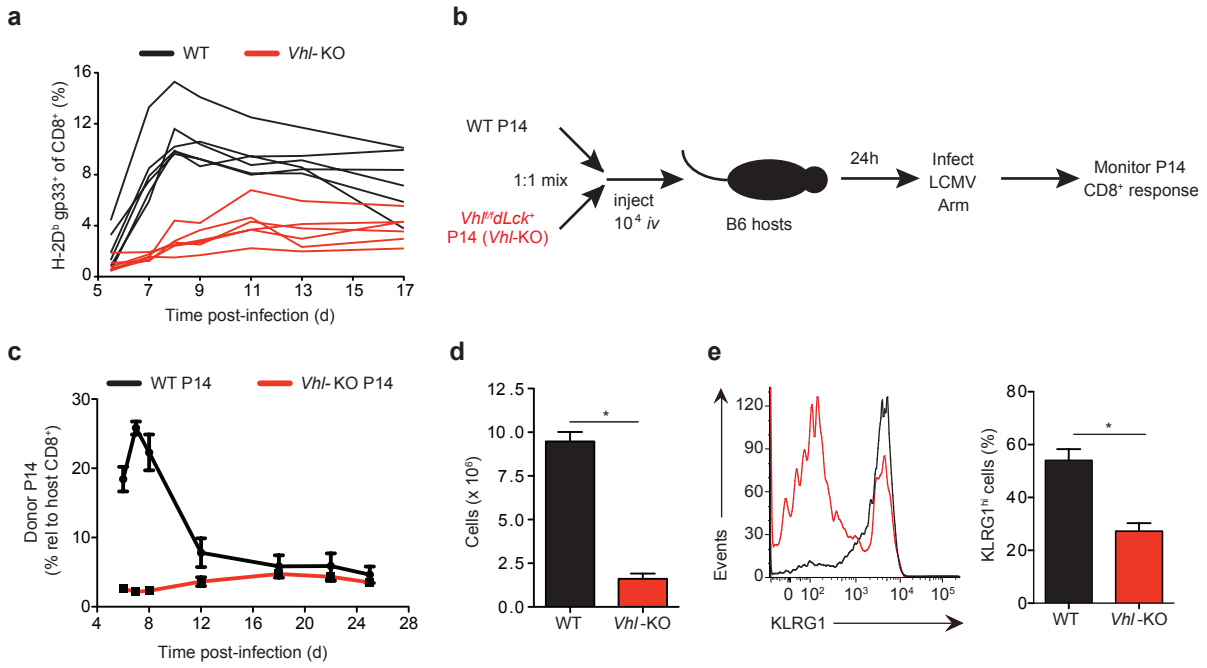

Supplementary Figure 3. VHL-sufficient and VHL-deficient CD8$^+$ T cell response to acute viral infection. (**a**) Wild-type or *Vhl*$^{fl/fl}$ dLck (VHL-KO) mice were infected with LCMV Armstrong and the CD8$^+$ T cell response in peripheral blood was monitored with MHC class I H-2D^b gp33 tetramers to detect LCMV-specific CD8$^+$ T cells. Each line indicates an individual mouse; n=6, representative of two experiments. (**b-e**), A 1:1 mixture of 10^4 VHL-sufficient and VHL-deficient P14 CD8$^+$ T cells were transferred to B6 hosts followed by infection with LCMV Armstrong one day later; n=3, error bars indicate s.e.m. (**b**) Experimental scheme. (**c**) Frequency of transferred VHL-sufficient and VHL-deficient P14 virus-specific cells in peripheral blood as a % of host CD8$^+$ T cells. (**d**) Absolute number of VHL-sufficient and -deficient P14 splenocytes on day 8 of infection, * P = 0.0002, (Student's unpaired t-test) (**e**) KLRG1 expression by VHL-sufficient and VHL-deficient P14 cells on day 7 of infection; n=3, * P = 0.007 (Student's unpaired t-test). Results representative of three independent experiments.

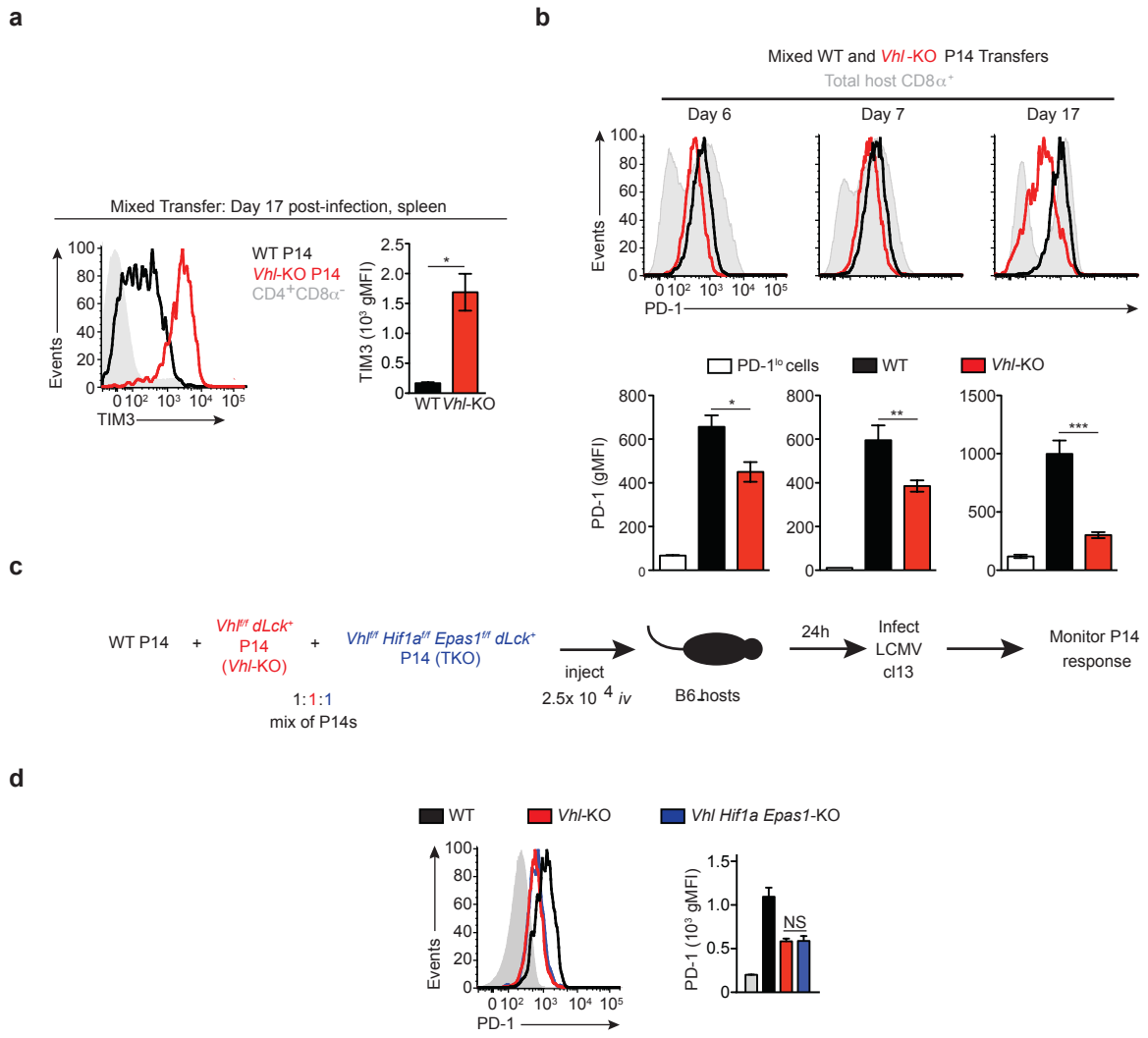

Supplementary Figure 4. Inhibitory and exhaustion-associated TIM-3 is increased on VHL-deficient cells and reduced PD-1 expression on VHL-deficient cells is HIF-1α-HIF-2α independent and VHL-dependent. (**a**) Cotransfer of VHL-sufficient and VHL-deficient P14 CD8$^+$ T cells followed by LCMV clone 13 infection as in Fig. 2a; histograms of TIM-3 expression and gMFIs of P14 CD8$^+$ T cells from spleen on day 17 of infection with LCMV clone 13; n=4, * P = 0.008 (Student's unpaired t-test). (**b**) Cotransfer of VHL-sufficient and VHL-deficient P14 CD8$^+$ T cells followed by LCMV clone 13 infection as in Fig. 2a; flow cytometric analysis of splenic VHL-sufficient P14 (black) or VHL-deficient P14 (red) CD8$^+$ T cells at the indicated time points, gMFI shown below. Expression of PD-1 on total host CD8α$^+$ T cells excluding P14 donor cells (histograms, grey), or gMFI for PD-1 low – expressing cells (in graphs, open bars) shown for reference; n=3, * P = 0.004, ** P = 0.05 and *** P = 0.004 (Student's unpaired t-test). (**c**) Experimental design for a mixed transfer of VHL-sufficient, VHL-deficient and VHL-HIF-1α-HIF-2α-triple-deficient P14 CD8$^+$ donor cells. (**d**) Histogram of each donor population displaying PD-1 (left) and gMFI graphed (right); peripheral blood on day 7 of infection; n=3, error bars indicate s.e.m.

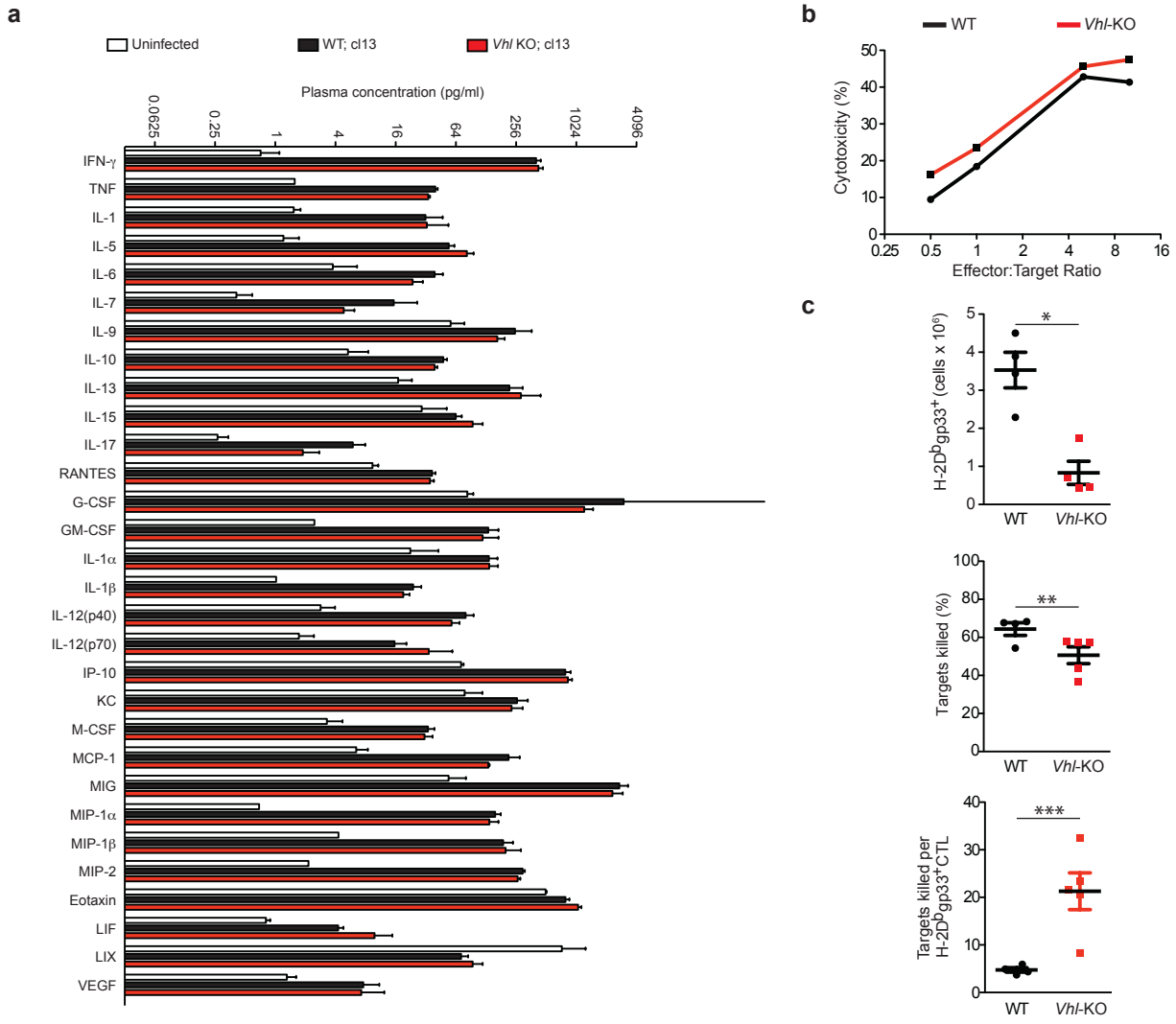

Supplementary Figure 5. Similar plasma cytokine levels in wild-type and $Vhl^{fl/fl}$ dLck mice responding to persistent infection and *in vitro* and *in vivo* cytotoxicity assays of VHL-sufficient and VHL-deficient cells responding to persistent infection. (**a**) Plasma cytokine levels in uninfected, polyclonal wild-type, or polyclonal $Vhl^{fl/fl}$ dLck on day 6 of infection with LCMV clone 13; uninfected n=2, wild-type n=5, $Vhl^{fl/fl}$ dLck n = 4; error bars indicate s.e.m. Cytokine levels were determined using Milliplex 32-plex premixed magnetic cytokine array and Luminex bead reader according to the manufacturers instructions. (**b**) *In vitro* cytotoxicity assay: VHL-sufficient P14 (here designated as WT) or VHL-deficient P14 T cells (VHL-KO) were transferred into B6 hosts that were then infected with LCMV clone 13 as in Fig. 1a. Splenocytes from hosts harboring VHL-sufficient or VHL-deficient P14 cells were enriched for $CD8^+$ cells on day 7 of LCMV clone 13 infection. Whole splenocytes from an uninfected mouse were used as targets; cells were coated with gp33-41 peptide (KAVYNFATC) at 1μm for one hour, labeled with 5μm of eFluor670 and mixed 1:1 with splenocytes labeled with 250nM of eFluor670. Appropriate numbers of VHL-sufficient or VHL-deficient P14 T cells were added to achieve effector to target ratios indicated, incubated with target cells for 4 hrs, and then assayed by flow cytometry. (**c**) *In vivo* cytotoxicity assay: VHL-sufficient versus VHL-deficient P14 T cells were transferred into B6 hosts and infected with LCMV clone 13. Whole splenocytes coated with or without gp33 peptide and eFluor670 labeled as in **b**, 2.5 x 10^6 gp33 peptide coated cells per mouse were injected *iv* 16 days after infection. One hour after injection of target cell mix, splenocytes were isolated from host mice and assayed by flow cytometry. The absolute number of cells binding H-$2D^b$ gp33 tetramer (top), the % killing of target cells (middle) and the approximate killing per antigen-specific $CD8^+$ T cell (bottom) are shown. To calculate targets killed per antigen-specific cell: the number of peptide-coated cells transferred to the infected host mouse was multiplied by the % killed to obtain an estimate of absolute number killed. The absolute number of target cells killed was then divided by the number of H-$2D^b$ gp33 $tetramer^+$ $CD8^+$ T cells per host spleen to approximate killing per cell. * P = 0.003, ** P = 0.05 and *** P = 0.007 (Student's unpaired t-test). Error bars indicate s.e.m. for all plots.

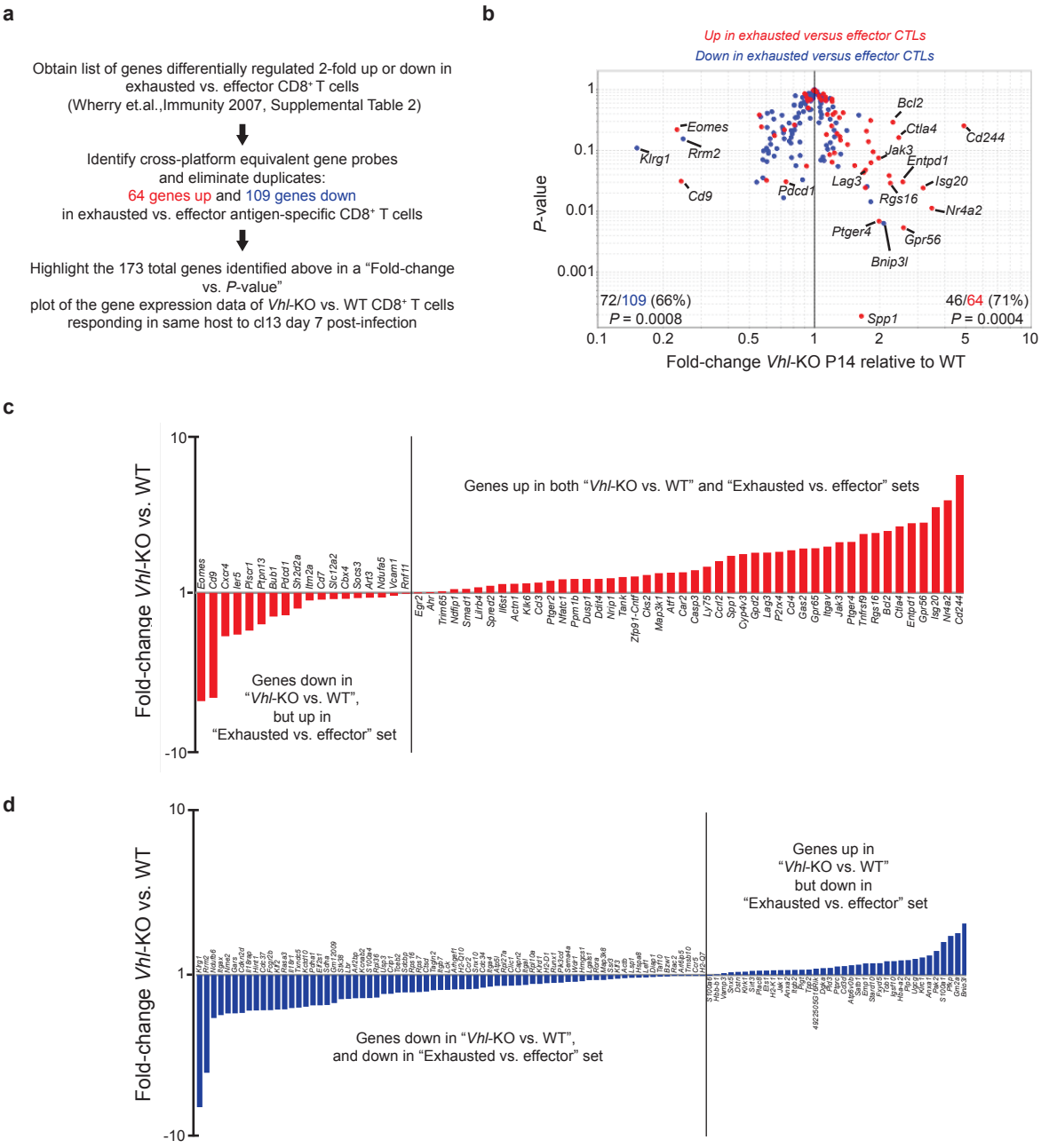

Supplementary Figure 6. Comparison of established "exhaustion gene-expression profile" with VHL-deficient-expression profile shows significant correlation, but identifies differently expressed genes. (**a**) Flow chart of analysis. (**b**) Fold-change versus *P*-value plot of VHL-deficient versus VHL-sufficient P14 cells at day 7 post-infection (data from Fig. 3a). Genes that were reported[1] to be upregulated in wild-type exhausted versus wild-type effector cells are highlighted in red, those down in blue; selected genes are identified. Genes up- or downregulated in VHL-deficient versus VHL-sufficient P14 cells show significant correlation with the genes previously reported to be up- or downregulated with exhausted versus effector cells (P = 0.0008 and 0.0004, respectively); Chi-squared test assuming equal distribution of genes up- and downregulated for the VHL-deficient versus VHL-sufficient and exhausted versus effector comparisons. (**c**) Bar graph representation of the data in **a,b** identifying the 64 genes that were upregulated in exhausted versus effector CTL; fold-change for VHL-deficient versus VHL-sufficient P14 cells is plotted. (**d**) As in **c**, but the fold-change expression of VHL-deficient versus VHL-sufficient of the 109 genes identified in **a,b** as being downregulated in exhausted versus effector cells.

Supplementary References:

1. Wherry, E.J., et al. Molecular signature of CD8+ T cell exhaustion during chronic viral infection. Immunity 27, 670-684 (2007).